

## SAS 3 OBSERVATIONS OF CYGNUS X-1: THE INTENSITY DIPS<sup>1</sup>

RONALD A. REMILLARD AND CLAUDE R. CANIZARES<sup>2</sup>

Department of Physics and Center for Space Research, Massachusetts Institute of Technology

Received 1982 October 4; accepted 1983 August 22

### ABSTRACT

X-ray light curves of Cyg X-1 are presented for three 3<sup>d</sup>-6<sup>d</sup> observations, each of which contains one or more intensity dips that are accompanied by spectral hardening. The dip profiles range from a smooth 8 hr event to a continual sequence of 10-100 minute dips that lasts for one-third of a (5<sup>d</sup>6) binary period. The dips generally occur near superior conjunction of the X-ray source, but one pair of 2 minute dips occurs when the X-ray source is nearer to the observer than is the supergiant companion. The dips are spectrally analyzed using seven energy channels in the range 1.2-50 keV. There is essentially no change in the spectral index during the dips. Reductions in the count rates are observed at energies greater than 6 keV for some of the dips, but the dip amplitude is always much greater in the 1.2-3 keV band. Absorption by partially ionized gas may best explain these results, given the observations of Pravdo *et al.* which rule out absorption by unionized material. Estimates are given for the intervening gas density, extent, and distance from the X-ray source. The problems confronting the models for the injection of gas through the line of sight, believed to be inclined by ~30° from the binary pole, are discussed.

*Subject headings:* stars: individual — X-rays: binaries

### I. INTRODUCTION

The analysis of X-ray intensity dips caused by increases in the column density along the line of sight is a primary source of information about the mass distribution in X-ray binary systems. Several X-ray sources show frequent but irregular intensity dips with accompanying spectral hardening, and in some cases the dips correlate with a particular orbital phase or show approximate periodicity that can help constrain the models for these mass-accreting systems (e.g., Crosa and Boynton 1980; Schreier *et al.* 1976; White and Swank 1982; Walter *et al.* 1982; Kallman and White 1982; Kahn 1982; White, Kallman and Swank 1982).

Cyg X-1 has frequently exhibited irregular, absorption-like intensity dips (Li and Clark 1974; Mason *et al.* 1974; Parsignault *et al.* 1976; Murdin 1976; Pravdo *et al.* 1980). These events have time scales from minutes to hours, and they occur preferentially near times of superior conjunction of the X-ray source.

There are outstanding obstacles to a clear understanding of these events. Unlike other binaries that exhibit dip phenomena, Cyg X-1 does not show X-ray eclipses, and has a probable inclination of 30°-40° (Bolton 1975; Guinan *et al.* 1979; Daniel 1981). Therefore, obscuring material must be far above the orbital plane. Second, the physical state of the obscuring material is not well determined. Pravdo *et al.* (1980) show that the X-ray spectrum during dips cannot be the result of absorption of the intrinsic spectrum by cold material. Similar spectral complexity is seen in the dips of other sources (e.g., Kallman and White 1982; White, Kallman, and Swank 1982).

Cyg X-1 was observed by the SAS 3 satellite on many occasions. The most extensive of these were 3<sup>d</sup>-6<sup>d</sup> pointed

observations during which the experiment was operated alternately in a normal and a high time resolution mode (modes A and B, respectively). We have detected variability at all measurable time scales. The results can be divided into two classes, each of which is extensively documented in the literature for Cyg X-1: intrinsic source variations (which includes continual rapid variability), and the intensity dips. In this paper, we exhibit and analyze the intensity dips that were recorded by SAS 3. Some high speed data were reported by Weisskopf *et al.* (1978), and further work is in progress.

### II. OBSERVATIONS

The SAS 3 detectors are mechanically collimated gas-filled proportional counters with sensitivity over the range 1-50 keV (see Buff *et al.* 1977; Lewin *et al.* 1976). In mode A operation counts are accumulated in intervals of 0.41 or 0.83 s in seven broad energy bands.

To study rapid fluctuations in X-ray intensity, SAS 3 has a high speed event monitor (HSEM) which is used in a single energy band (mode B operation). A set of coaligned detectors is selected, and their full energy response defines the bandwidth in which data are collected. After the satellite's usual anticoincidence screening, a 4096 bit memory registers whether or not a photon is received from any of the selected detectors during a sampling time, which can be set to (approximately) 8.0, 1.0, or 0.125 ms. Once the memory is filled, data recording is interrupted in order to write the contents into the telemetry stream and set up the next sequence. As a result, each 4096 bit HSEM record is an independent, continuous, source observation. The system's binary response requires the selection of detectors and sampling time that provide a data rate that is well below saturation.

The satellite's orientation is monitored with a star-camera system, and transmission corrections for the system's collimators have been empirically confirmed. The detectors

<sup>1</sup> This research was supported in part by NASA under contract NAS-5-24441.

<sup>2</sup> Alfred P. Sloan Research Fellow.

remain in operation during Earth occultation, providing X-ray background measurements. The full amplitude of the background variations was less than 10% for every energy channel, and the mean background rates agreed with off-target pointed observations to within a few percent. At maximum transmission the source rate is a factor of 6–15 above background for the three energy channels which scan 1.5–12 keV and a factor of 1–3 above background for the remaining energy channels.

This paper includes results from observations taken on 1976 August 4–7, 1976 October 10–14, and 1977 August 10–16. During these times, the SAS 3 system was used in both modes A and B. In a typical satellite orbit (~100 minutes) the source was acquired after Earth occultation and measured for ~5 minutes in mode A. The system was then switched to mode B, and HSEM data were collected for ~50 minutes. Finally, there was a return to mode A operation for another 5 minute measurement before Earth occultation began. We have excluded data taken when the collimator transmission was less than 40% and when the satellite encountered the high particle flux at the South Atlantic Anomaly.

Spectral fits are calculated by a program that iterates a minimum  $\chi^2$  solution for a power-law relation

$$I(E)dE = I_0 \exp[-(E_a/E)^{2.67}]E^{-a}dE, \quad (1)$$

where  $I(E)$  is the flux in photons  $\text{cm}^{-2} \text{s}^{-1} \text{keV}^{-1}$ ,  $E_a$  is the cutoff energy, and  $a$  the spectral index. Test parameters are chosen, and the resulting spectrum is folded over the energy response function of each selected detector, generating a model count rate. Free spectral parameters are adjusted until  $\chi^2$  is minimized, and the column density is calculated from the cutoff energy using cross sections calculated by Brown and Gould (1970). These cross sections refer to photoelectric absorption by cold material. As discussed below, the absorbing material is at least partially ionized; if so, the deduced column densities are probably about one-half the true values (Tarter, Tucker, and Salpeter 1969).

### III. RESULTS

Intensity dips with accompanying spectral hardening were found during each of three long-term observations in which Cyg X-1 was in its “low” state (the source occasionally exhibits “high” states of 1 month or longer duration in which the soft X-ray emission is greatly increased; see Oda *et al.* 1976). In Figures 1–3 the overall light curves for mode A data are shown, corrected for aspect and background rates. Count rates are displayed in two energy bands, and the data are from the “horizontal” tubular collimated detector (HT) and the “xenon” tubular collimated detectors (XT). The spectral hardness is defined as the ratio of the 6–27 keV HT and XT source counts to those in the 1.2–3 keV HT energy channel, with the exception of the 1976 August observation for which the 6–12 keV and 1.2–3 keV HT energy channels are used since the XT was turned on only after the intensity dip minimum had occurred. The apparent spectral stability of the source during flares in which the intensity increases by up to 60% contrasts with the spectral hardening that is evident during the intensity dips.

In Figure 1 there is a major dip centered near 1976 August 4.3. This event is shown with greater time resolution in mode B data (corrected source counts, 2–12 keV bandwidth) shown

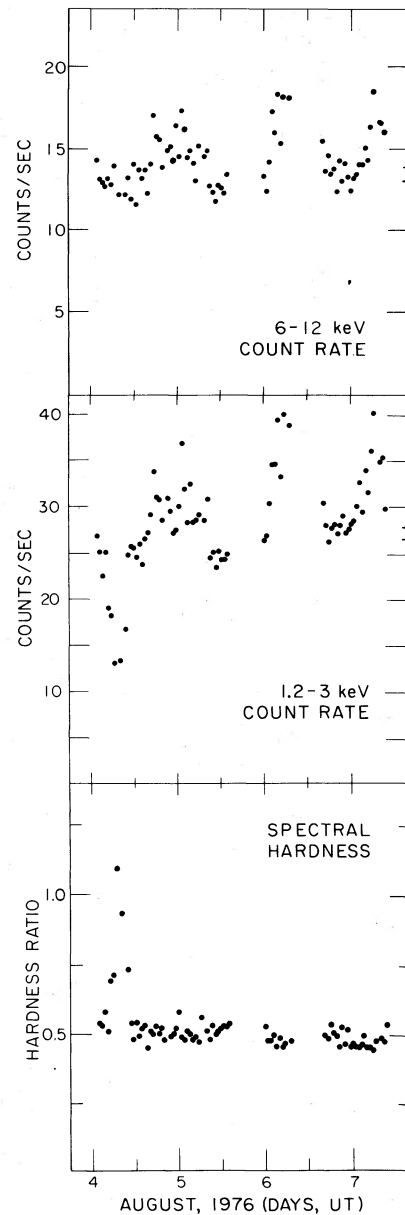


FIG. 1.—Cyg X-1 count rates and hardness ratio from mode A data (5% duty cycle) obtained during 1976 August. In the ephemeris of Gies and Bolton (1981) superior conjunction of the X-ray source occurred on August 4.16.

in Figure 4. The dip is an extremely long one for Cyg X-1 (~8 hr) and there is little evidence of structure at shorter time scales. The dip depth has a fractional amplitude of  $0.46 \pm 0.03$  in the 1.2–3 keV energy channel. A very similar broad dip is seen in the 3–6 keV energy channel, but with a depth of  $0.18 \pm 0.05$ . The event is not detected in energy channels greater than 6 keV. In the ephemeris of Gies and Bolton (1982) the binary period of Cyg X-1 is very nearly  $5^d.6$  and superior conjunction occurs on  $\sim 4^h \pm 0^m.5$  UT on 1976 August 4. This places the dip minimum at orbital phase  $0.03 \pm 0.02$  (the phase is defined to be zero at superior conjunction of the X-ray source).

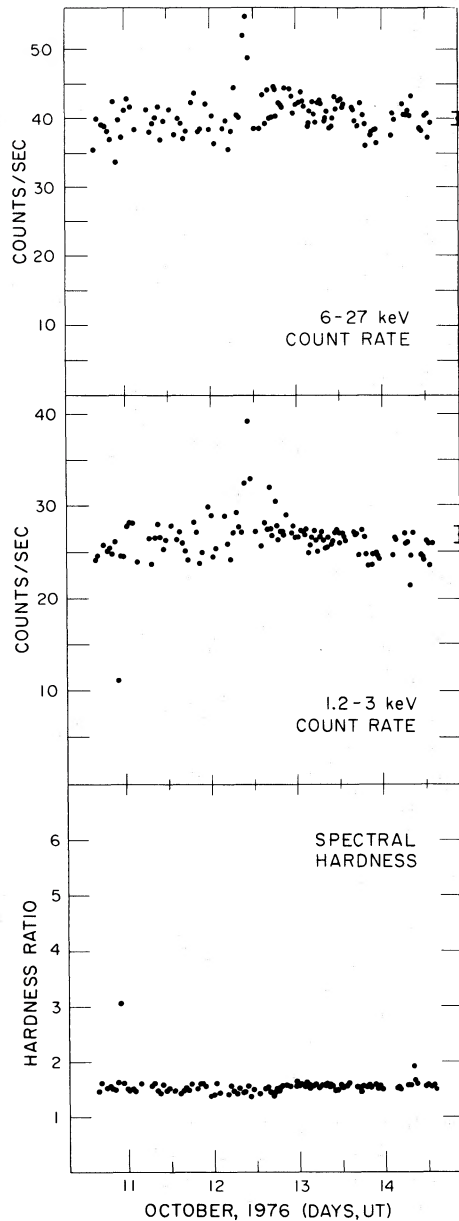


FIG. 2.—Cyg X-1 count rates and hardness ratio from mode A data obtained during 1976 October. Superior conjunction of the X-ray source occurred on October 10.36 (Gies and Bolton 1981).

Figure 2 contains the 1976 October results and two indications of every short-lived intensity dips. In this observation mode B operation was suspended after October 12.6, and this accounts for the higher density and decreased scatter of data points for that portion of the mode A light curve (Fig. 2). The dip near October 10.9 occurs at orbital phase  $0.09 \pm 0.02$  and has a duration of less than 50 but greater than 3 minutes. Unfortunately, the high speed data taken during the event was selected with a 6–27 keV bandwidth, and there is no record of the dip profile. The second event occurs on October 14.3, and the detection is marginal in Figure 2. However, further investigation has revealed that two significant and very brief ( $\sim 2$  minutes) dips occurred

within that exposure time, and this is shown with 20 s time resolution in Figure 5. The pair has an orbital phase of  $0.71 \pm 0.02$  (Gies and Bolton 1982), and this marks the first detection of absorption-like events while the X-ray source is nearer to the observer than is the O9.7 supergiant primary star.

All of these events are also seen with smaller amplitude in the lowest energy channel (2–6 keV) of the slat-collimated detectors, confirming the results in Figures 1–5, which utilize the 1.2–3 keV energy channel of the HT detector.

The 1977 August observation, shown in Figure 3, contains the most active exhibition of dip phenomena reported for

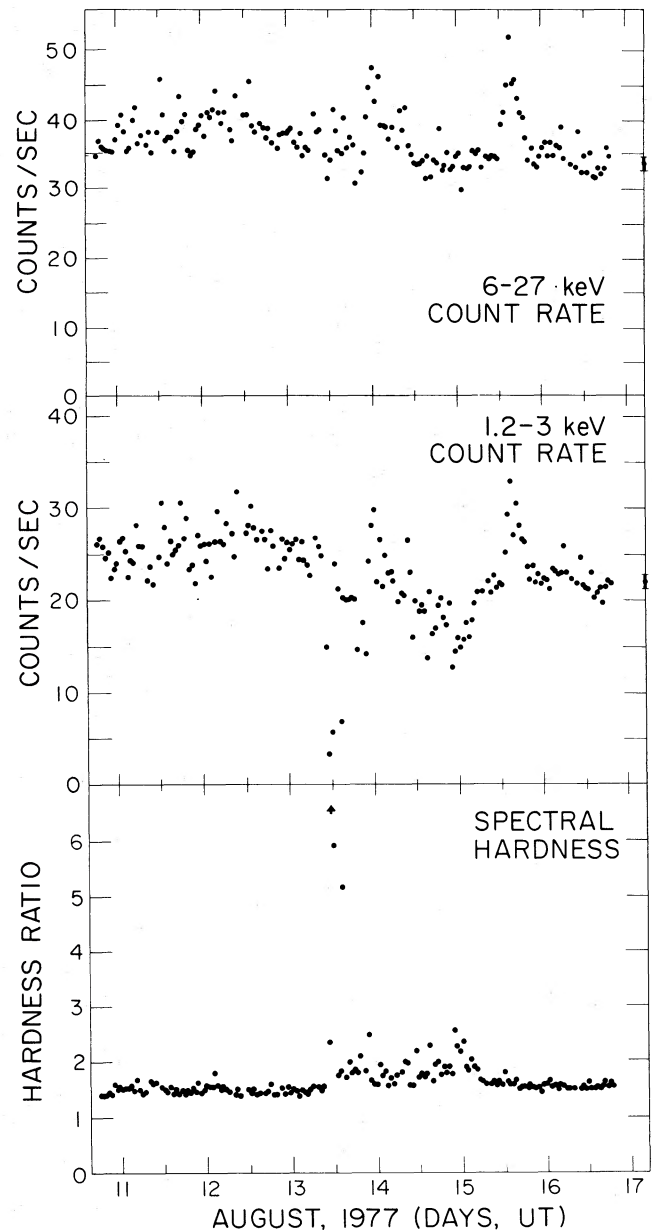


FIG. 3.—Cyg X-1 count rates and hardness ratio from mode A data obtained during 1977 August. Superior conjunction of the X-ray source occurred on August 14.35 (Gies and Bolton 1981), which is near the center of 1<sup>st</sup> of dip activity. The arrow in the hardness ratio plot designates a value (8.1) that is beyond the plot range.

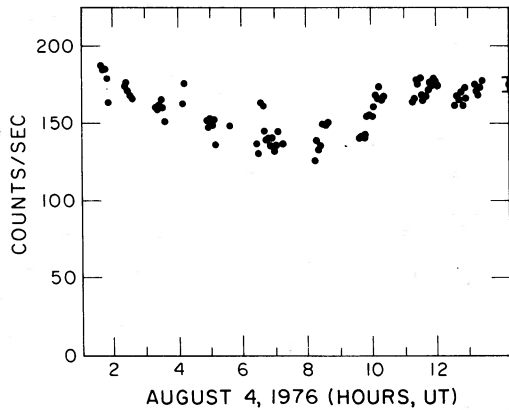


FIG. 4.—1976 August intensity dip shown with 3.6 minute time resolution, using data from both modes A and B.

Cyg X-1. Superior conjunction occurred on August 14.35, which is near the center of the period of spectral hardness variability. The continual  $3-10\sigma$  variations cover 1<sup>9</sup> (orbital phases 0.81–0.15), with dip time scales ranging from minutes to several hours. There are some extremely sharp intensity dips near the onset of this period, and they are exhibited with mode B data in Figure 6. Higher time resolution (20 s) of the three data segments having the steepest gradients is shown in Figure 7. Here it is seen that the events are dominated by sharp features with time scales from 2–10 minutes, in marked contrast to the much smoother event of 1976 August.

Spectral fits were calculated for data points in Figures 1–3, using seven energy channels which span 1.2–50 keV (see § II). The calculation assumes a power-law spectrum (see Nolan *et al.* 1981; Steinle *et al.* 1982) and photoelectric absorption parametrized by the equivalent column density for absorption by neutral material. Fifteen intensity dip minima were analyzed, and a consistent pattern of results was obtained. The deduced column density increases significantly during the

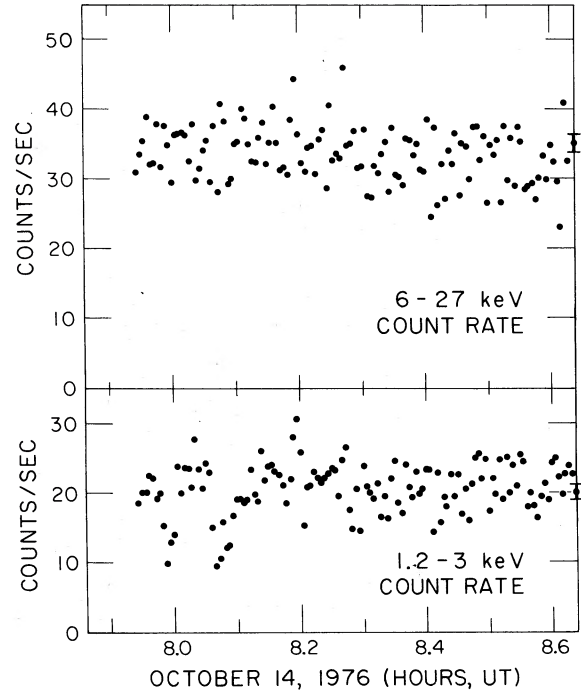


FIG. 5.—Dip of 1976 October 14.35 (see Fig. 2) shown with 20 s time resolution (mode A data). This data interval has an orbital phase of  $\sim 0.71$ .

intensity dips, and these changes appear very similar to the spectral hardness plots in Figures 1–3. In contrast, the spectral index is marginally smaller (indicating a harder spectrum) by an amount  $\leq 0.1$  during the deepest intensity dips, but with only  $2\sigma$  significance. There are occasions when the energy channels above 6 keV appear reduced by as much as 28% (compared to 90% in the 1.2–3.0 keV band), but the spectral index is not substantially changed. This result, shown in Figure 8, confirms the statement by Pravdo *et al.* (1980) that the flattening of the spectra during the intensity dips is not

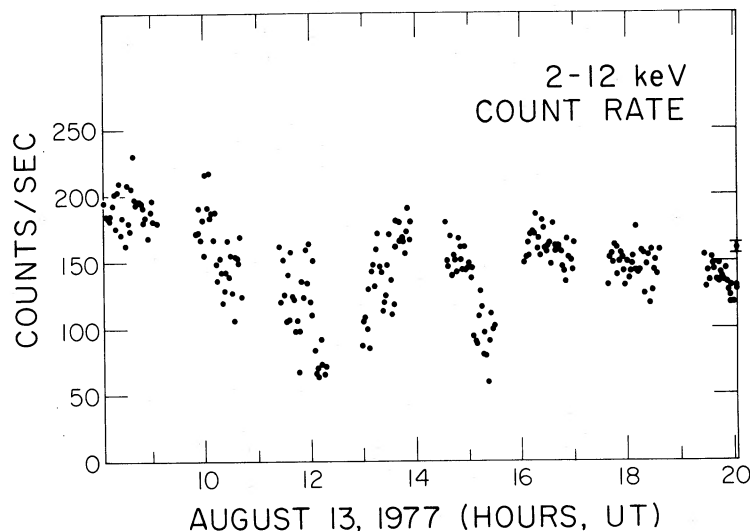


FIG. 6.—Sharp intensity dips of 1977 August using data from both modes A and B. The three intervals between 11<sup>h</sup> and 16<sup>h</sup> UT are shown with higher time resolution in Fig. 7.

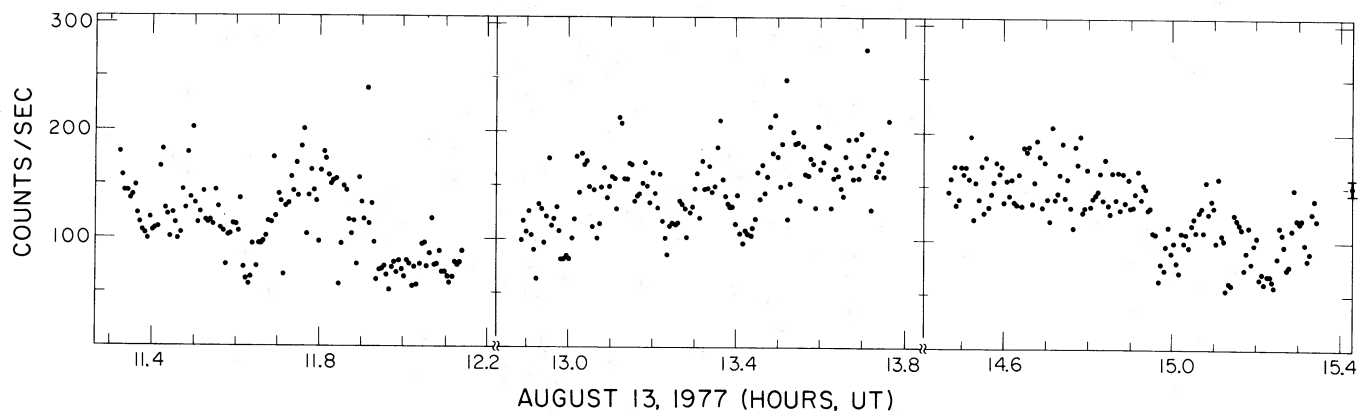


FIG. 7.—Sharp dips of 1977 August shown at 20 s time resolution, revealing at least six individual dips having time scales of 2–10 minutes

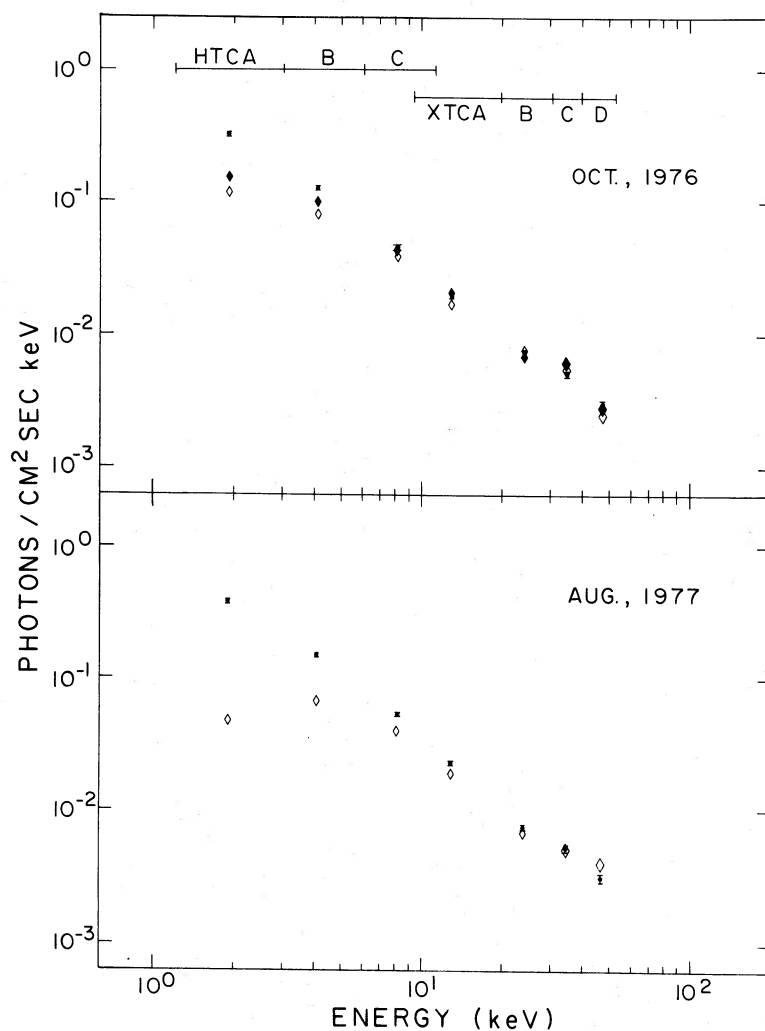


FIG. 8.—X-ray spectra during normal states (filled circles with error bars) and intensity dip minima (filled and open diamonds, vertically scaled to  $\pm 1 \sigma$  values). The full bandwidth for each energy channel is plotted above the data. The top section exhibits the sharp dip (open diamonds) and the narrow dips at orbital phase 0.71 (filled diamonds) observed in 1976 October, and the lower section shows the mean spectrum of four very sharp and similar dips observed in 1977 August.

TABLE 1

## A. INTENSITY DIP ANALYSIS

"Normal" Spectral Parameters	1976 Aug	1976 Oct	1977 Aug
Number of measurements .....	17	20	30
Orbital phase ( $\pm 0.02$ ) .....	0.15-0.56	0.15-0.70	0.20-0.90
Spectral index (number) .....	1.605(0.031)	1.474(0.047)	1.499(0.030)
Equivalent column density ( $10^{21} \text{ cm}^{-2}$ ) .....	2.49(1.51)	2.60(2.05)	3.94(1.30)
Reduced $\chi^2$ .....	1.56(0.95)	1.65(0.91)	0.81(0.61)

## B. INTENSITY MINIMA

Parameter	Broad Dip (1976 Aug)	Sharp Dip (1976 Oct)	Narrow Dips (1976 Oct)	Sharp Dips (1977 Aug)	Secondary Dips (1977 Aug)
Structure .....	one 8 <sup>h</sup> dip	? 3-5 <sup>m</sup>	double 1.7, 2 <sup>m</sup> 5	complex many minima	10-100 <sup>m</sup> for 1 <sup>d</sup> 9
Time (UT) .....	1976 Aug 4.3	1976 Oct 10.90	1976 Oct 14.34	1977 Aug 13.51	1977 Aug 14
Number of fits calculated .....	4	1	2	7	4
Average exposure time (min) .....	1.1	2.1	2.1	1.3	2.8
Orbital phase .....	0.03	0.10	0.71	0.85	0.89-0.11
Spectral index .....	1.62(0.04)	1.36(0.06)	1.38(0.06)	1.43(0.05)	1.49(0.05)
Density ( $10^{21} \text{ cm}^{-2}$ ) .....	29.2(6.4)	21.5(5.1)	20-33(6.9)	44-86(11.0)	13-26(3.6)
Reduced $\chi^2$ .....	1.18(0.40)	1.28	0.95(0.46)	0.86(0.52)	0.98(0.42)
Dip depth (1.2-3 keV) .....	0.46(0.03)	0.64(0.03)	0.53(0.07)	0.67-0.88(0.04)	0.39-0.47(0.04)
Dip depth (3-6 keV) .....	0.18(0.05)	0.36(0.04)	0.23(0.05)	0.29-0.52(0.04)	0.20-0.27(0.04)
Dip depth (6-12 keV) .....	<0.05	0.16(0.05)	<0.06	0.13-0.28(0.05)	0.05-0.19(0.05)
Dip depth (8-27 keV) .....	...	0.05(0.05)	<0.00	0.03-0.18(0.05)	0.10(0.05)

observed at energies greater than 5 keV. Cyg X-1 dip analyses that were confined to spectral ranges between 1 and 7 keV (Pravdo *et al.* 1980; Parsignault *et al.* 1976) show the spectral index to change by 0.5 to 1.2 units.

A summary of our results is provided in Table 1. This includes a dip ephemeris, the calculated spectral parameters during dips and normal states, and the fractional reductions in source count rates at dip minima for selected energy bands. The spectral parameters at the intensity minima are averaged when a number of similar dips occurred in succession, and the listed uncertainties in those cases are the sample standard deviations for the indicated number of calculations. The minimum of the 8 hr dip of 1976 August was spectrally analyzed in four sections separately, and no significant deviations were found among them. Finally, during  $\sim 1^d9$  of dip activity observed during 1977 August, the column density is always greater than  $7 \times 10^{21} \text{ cm}^{-2}$ , which is more than twice the value obtained at other "normal" times.

## IV. DISCUSSION

The intensity dips shown here demonstrate the frequency and complexity of this type of event in X-ray observations of Cyg X-1. The correlation between the dips and superior conjunction of the X-ray source is basically confirmed, but the phenomenology of these events has been expanded by the detection of weak events at an orbital phase of 0.71, the measurement of a range of 2 minutes to 8 hr in intensity dip time scales, and the observed aggregation of brief dips that extended over 1<sup>d</sup>9 or one-third of an orbital period. The intensity depressions with long time scales (0<sup>d</sup>3, 1<sup>d</sup>9) are centered very near superior conjunction of the X-ray source, and similar variations may have produced the 5<sup>d</sup>6 modulation detected in the *Ariel 5* scanning observations (3-6 keV) by Holt *et al.* (1976). The intensity dips are

clearly beyond explanation by simplified accretion models (e.g., steady-state thin disk or wind accretion; see Bolton 1975), but the characteristics and the location of the mass causing these events are yet to be established.

Our spectral analysis of the dips requires an X-ray cross section that is markedly more efficient at low (1.2-3 keV) X-ray energies. Our coarse resolution does not permit sophisticated modeling of the dips, but the extent (1.2-50 keV) of the total energy coverage contributes useful information. The high resolution spectra (0.8-4 keV) obtained by Pravdo *et al.* (1980) during two dips exclude photoelectric absorption of a fixed power law by cold matter. Pravdo *et al.* suggest that the spectral hardening below 4 keV seen in the dips may result from Comptonization of the emergent photons by a blob of  $\sim 5$  keV electrons with significant electron scattering optical depth along the line of sight. They do not actually model such a spectrum. Comptonization calculations of a power-law spectrum scattered by thermal electrons by Illarionov and Sunyaev (1972), Sunyaev and Titarchuk (1980), and others suggest that such a flattening would indeed occur at energies less than 10 keV if the blob has a large optical depth relative to Thompson scattering. However, these authors also show that such a significant flattening ( $\sim 1$  unit change in the spectral index) of the spectrum at energies below the mean electron energy would be accompanied by a very steepened spectrum at higher energies (e.g., greater than 20 keV). We detect no sign of this effect (see Fig. 8).

It may be possible to reconcile these observations if the absorbing material is partially ionized. Spectral distortions during the dips would then be confirmed to low energies, but the photoelectric cross section of this material would be suppressed, especially at the lowest observed X-ray energies, compared to absorption by neutral gas. Such an explanation has been invoked to explain similar dip spectra in Vela X-1

(Kallman and White 1982) and 4U1700–37 (White, Kallman, and Swank 1982). White, Kallman, and Swank also suggested that the SSS data of Pravdo *et al.* (1980) on Cyg X-1 might be explained in this way. For the strongest dips (e.g., 1977 August) electron scattering opacity might also be a factor. Pravdo *et al.* (1980) considered absorption by partially ionized material. They did not favor it because a model with SiK, SK, and FeL absorption edges gave a poor fit to the data. However, absorption in partially ionized material is not necessarily dominated by these edges, so their fits do not rule it out. This can be seen from the models of Hatchett, Buff, and McCray (1976) and Kallman and McCray (1982), who consider the transfer of X-rays through partially photoionized gas (e.g., see Fig. 5a of Hatchett, Buff, and McCray 1976; for a small absorbing blob along the line of sight, the continuum shape would resemble that shown but the emission lines would be absent). The details of which edges might be present depend on the ionization state of the gas.

The cloud parameters can be estimated as follows. Partial ionization implies that the ionization parameter  $\xi = L/nr^2$  is  $10\text{--}10^3$  (Tarter, Tucker, and Salpeter 1969;  $L$  is the X-ray luminosity in  $\text{ergs s}^{-1}$ ,  $n$  the cloud density in  $\text{cm}^{-3}$ , and  $r$  the cloud distance from the X-ray source in cm). If the absorbing cloud is more or less spherical and has a fixed position in the binary system, then  $\xi$  can be expressed

$$\xi = 2\pi Lt(NPr)^{-1}, \quad (2)$$

where  $t$  is the characteristic duration of a dip,  $N$  is the column density of the blob, and  $P$  is the orbital period of Cyg X-1. Using  $L \approx 10^{37}$   $\text{ergs s}^{-1}$ ,  $N \approx 6 \times 10^{22}$   $\text{cm}^{-2}$ , which is about twice the equivalent neutral hydrogen column density from Table 1 (see § II and Tartar, Tucker, and Salpeter 1969), and  $P = 5^d6$ , one finds  $r \approx 10^{10}$  ( $t/5$  minutes) ( $\xi/100$ ) $^{-1}$  cm. This becomes a lower limit if, as is likely, the cloud has a nonzero velocity in the corotating frame. It implies that the cloud size is greater than  $2 \times 10^7$  ( $t/5$  minutes) $^2$  ( $\xi/100$ ) $^{-1}$  cm, and that  $n \leq 10^{15}$  ( $t/5$  minutes) $^{-2}$  ( $\xi/100$ ) $\text{cm}^{-3}$ .

The injection mechanism of the intervening mass is a second unresolved question. The association of the dips with orbital phases near zero initially suggested occultation by a stream

of matter resulting from Roche lobe overflow (Li and Clark 1974; Mason *et al.* 1974; Murdin 1976). Portions of this stream would have to be displaced far above the orbital plane if it is to intercept the line of sight in a system with a probable inclination of  $30^\circ\text{--}40^\circ$  (Bolton 1975; Guinan *et al.* 1979; Daniel 1981). Lubow and Shu (1976) consider the dynamics of the interaction between a mass stream and a dense accretion disk. They find that a bow shock forms, deflecting some material perpendicular to the disk plane. This material may then circulate within the Roche lobe before becoming entrained in the disk. With a nonsteady accretion stream (see Bolton 1975), this mechanism can account for many aspects of the Cyg X-1 dips, but there is not a clear explanation for the frequent multiple minima, nor the duration (one-third of an orbital period) of dip activity shown in Figure 3.

Mass transfer by Roche lobe overflow is implied by the phase-shifted radial velocity curve for the He II  $\lambda 4686$  emission line, taken to indicate the presence of a gas stream (Hutchings *et al.* 1973). However, wind accretion may be substantial (see Eardley *et al.* 1978), since UV and IR data reveal the existence of a reasonably robust wind (Treves *et al.* 1980; Persi *et al.* 1980). It is conceivable that a strong wind may also contribute to the injection of the intervening mass by increasing the scale height of deflected material or by causing prominences on the disk itself.

Finally, density enhancements in the wind itself could be causing the absorption. Such enhancements might result from shocks that form both downstream and upstream from the X-ray source (e.g., Fransson and Fabian 1980; Lucy 1982; Eadie *et al.* 1975) and have often been invoked to explain dip phenomena in eclipsing systems with OB primaries. Many of the ambiguities and complexities of the Cyg X-1 dips are also seen in those objects (e.g., Kallman and White 1982; White, Kallman, and Swank 1982).

We are grateful for the assistance of the SAS 3 group at the MIT Center for Space Research, and we thank C. T. Bolton and D. R. Gies for contributing their Cyg X-1 orbital ephemeris prior to publication.

#### REFERENCES

- Bolton, C. T. 1975, *Ap. J.*, **200**, 269.  
 Brown, R. L., and Gould, R. J. 1970, *Phys. Rev. D.*, **1**, 2252.  
 Buff, J., *et al.* 1977, *Ap. J.*, **212**, 678.  
 Crosa, L., and Boynton, P. E. 1980, *Ap. J.*, **235**, 999.  
 Daniel, J. Y. 1981, *Astr. Ap.*, **94**, 121.  
 Eadie, G., Peacock, A., Pounds, K. A., Watson, M., Jackson, J. C., and Hunt, R. 1975, *M.N.R.A.S.*, **172**, 35p.  
 Eardley, D. M., Lightman, A. P., Shakura, N. I., Shapiro, S. L., and Sunyaev, R. A. 1978, *Comments Ap.*, **7**, 151.  
 Fransson, C., and Fabian, A. C. 1980, *Astr. Ap.*, **87**, 102.  
 Gies, D. R., and Bolton, C. T. 1982, *Ap. J.*, **260**, 240.  
 Guinan, E. F., Dorren, J. D., Siah, M. J., and Koch, R. H. 1979, *Ap. J.*, **229**, 296.  
 Hatchett, S., Buff, J., and McCray, R. 1976, *Ap. J.*, **206**, 847.  
 Holt, S. S., Bildt, E. A., Serlemitsos, P. J., and Kaluzienski, L. J. 1976, *Ap. J. (Letters)*, **203**, L63.  
 Hutchings, J. B., Crampton, D., Glaspey, J., and Walker, G. A. H. 1973, *Ap. J.*, **182**, 549.  
 Ilarionov, A. J., and Sunyaev, R. A. 1972, *Soviet Astr.—AJ*, **16**, 45.  
 Kahn, S. M. 1982, Smithsonian Astrophysical Observatory preprint.  
 Kallman, T. R., and McCray, R. 1982, *Ap. J. Suppl.*, **50**, 263.  
 Kallman, T. R., and White, N. E. 1982, *Ap. J. (Letters)*, **261**, L35.  
 Lewin, W. H. G., Li, F. K., Hoffman, J. A., Doty, J., Buff, J., Clark, G. W., and Rappaport, S. 1976, *M.N.R.A.S.*, **177**, 93P.  
 Li, F. K., and Clark, G. W. 1974, *Ap. J. (Letters)*, **191**, L27.  
 Lubow, S. H., and Shu, F. H. 1976, *Ap. J. (Letters)*, **207**, L53.  
 Lucy, L. B. 1982, *Ap. J.*, **255**, 286.  
 Mason, K. O., Hawkins, F. J., Sanford, P. W., Murdin, P., and Savage, A. 1974, *Ap. J. (Letters)*, **192**, L65.  
 Murdin, P. 1976, in *X-ray Binaries*, ed. E. Boldt and Y. Kondo (NASA SP-389), p. 425.  
 Nolan, P. L., Gruber, D. E., Knight, F. K., Matteson, J. L., Rothschild, R. E., Marshall, F. E., Levine, A. M., and Primini, F. A. 1981, *Nature*, **293**, 275.  
 Oda, M., Doi, K., Ogawara, Y., Takagishi, K., and Wada, M. 1976, *Ap. Space Sci.*, **42**, 223.  
 Parisignault, D. R., Grindlay, J. E., Schnopper, H., Schreier, E. J., and Gursky, H. 1976, in *X-ray Binaries*, ed. E. Boldt and Y. Kondo (NASA SP-389), p. 429.  
 Persi, P., Ferrari-Toniolo, M., Grasdalen, G. L., and Spada, G. 1980, *Astr. Ap.*, **92**, 238.  
 Pravdo, S. H., White, N. E., Kondo, Y., Becker, R. H., Boldt, E. A., Holt, S. S., Serlemitsos, P. J., and McCluskey, G. E. 1980, *Ap. J. (Letters)*, **237**, L71.  
 Priedhorsky, W., Garmire, G. P., Rothschild, R. E., Boldt, E., Serlemitsos, P., and Holt, S. 1979, *Ap. J.*, **233**, 350.  
 Schreier, E. J., Swartz, K., Giacconi, R., Fabbiano, G., and Morin, J. 1976, *Ap. J.*, **204**, 539.  
 Steinle, H., Voges, W., Pietsch, W., Reppin, C., Trumper, J., Kendziorra, E., and Stauber, R. 1982, *Astr. Ap.*, **107**, 350.  
 Sunyaev, R. A., and Titarchuk, L. G. 1980, *Astr. Ap.*, **86**, 121.  
 Tarter, C. B., Tucker, W. H., and Salpeter, E. E. 1969, *Ap. J.*, **156**, 943.

Treves, *et al.* 1980, *Ap. J.*, **242**, 1114.

Walter, F. M., Bowyer, S., Mason, K. O., Clarke, J. T., Henry, J. P.,

Halpern, J., and Grindlay, J. E. 1982, *Ap. J. (Letters)*, **253**, L67.

White, N. E., Kallman, T. R., and Swank, J. H. 1982, *Ap. J.*, **269**, 264.

White, N. E., and Swank, J. H. 1982, *Ap. J. (Letters)*, **253**, L61.

Weisskopf, M. C., Sutherland, P. G., Katz, J. I., and Canizares, C. R. 1978,

*Ap. J. (Letters)*, **223**, L17.

CLAUDE R. CANIZARES and RONALD A. REMILLARD: MIT Center for Space Research, Room 37-535, Cambridge, Ma 02139